



Reproducible low-cost flexible quadruple-tank process experimental setup for control educators, practitioners, and researchers



Leonardo Pedrosa*, Pedro Batista

Institute for Systems and Robotics, Instituto Superior Técnico, Universidade de Lisboa, Portugal

ARTICLE INFO

Article history:

Received 23 May 2022

Received in revised form 20 July 2022

Accepted 22 August 2022

Available online xxxx

Dataset link: <https://github.com/decenter2/021/quadruple-tank-setup>

Keywords:

Experimental setup
Quadruple-tank process
Industrial process
Control laboratory
Control education

ABSTRACT

The major hurdle in accessing laboratory experimentation is the cost of acquiring experimental scientific equipment, which is unbearable for many institutions. This paper aims to provide the community of control educators, practitioners, and researchers with an open-source low-cost experimental setup and dedicated interface, which is flexible and very easily reproducible. The proposed apparatus is a setup of four interconnected tanks. The setup is representative of real-life industrial processes and it can be adjusted to allow for several configurations for flexibility. A user-friendly dedicated MATLAB/Simulink interface with a personal computer is developed. It supports a seamless shift between a numeric simulation of the quadruple-tank process dynamics and the interface with the physical experimental plant. The CAD models, technical drawings, wiring schematics, PCB design, interface, assembly tutorials, and several examples are provided in an open-source repository. The parts are inexpensive, readily obtained, and fast to assemble. Each setup costs under 650€ and takes roughly 4 h to assemble. In this paper, several application examples are presented, not only for educational purposes, but also for the validation of a state-of-the-art decentralized control method.

© 2022 The Author(s). Published by Elsevier Ltd. This is an open access article under the CC BY-NC-ND license (<http://creativecommons.org/licenses/by-nc-nd/4.0/>).

1. Introduction

The use of meaningful experimental setups is an important tool of bridging the gap between theory and practice in complex control and automation systems. It is recognized to complement and enhance control education, illustrating theoretical concepts and providing a contextual setting. It is also a platform to validate and assess the performance of new automation approaches and control techniques for technicians and researchers. As a result, some attention has been given to this topic over the past decades, with the development of user-friendly real-time simulation tools [1,2] and of meaningful experimental setups [3–10]. These apparatuses ought to: (i) be meaningful and representative of real-life complex systems; (ii) be flexible, to allow for the simulation of various configurations and control techniques; (iii) have a user-friendly interface with standard numerical analysis software; and (iv) be reproducible, to allow for the validation of the obtained results. More recently, with the rise of the *Internet of Things*, many institutions are resorting to virtual web-based laboratory environments [11,12]. On one hand, this approach is very compelling because it is cheaper, easier to implement, and it allows remote access. On the other hand, the classic hands-on approach allows for a closer contact, which is fundamental in control education for acquiring practical experience and intuition.

The major hurdle in accessing laboratory experimentation is the cost of acquiring experimental scientific equipment, which is unbearable for many institutions that struggle for funding. This issue is holding back the success of control education and experimental validation of novel techniques. Furthermore, although research has been published detailing and exemplifying the use of novel experimental setups, the reader is often not provided with the necessary data, files, and software to be able to reproduce such apparatuses. In this context, some alternatives to traditionally prohibitively expensive experimental setups have been proposed for heat transfer [13–15] and control demonstrations [16–20], for instance. Recently, some low-cost apparatuses have been proposed leveraging 3D printing [18,21,22]. This paper aims to provide the community of control educators, practitioners, and researchers with an open-source low-cost experimental setup and interface, which is flexible and very easily reproducible. The proposed apparatus is a setup of four interconnected tanks inspired in the quadruple-tank process put forward in [3]. This setup is analogous to various industrial processes, whose automation allows for a more efficient, safer, and more profitable operation. The main purpose of [3] was to propose an experimental setup to illustrate performance limitations due to multivariate right half-plane zeros. Unfortunately, the experimental setup proposed therein was not designed to be reproducible, low-cost, or flexible. In fact, in [3]: (i) the details of the physical setup are omitted, namely the kind of sensors, pumps, valves, and data acquisition board, which hinders its reproduction; (ii) the user

* Corresponding author.

E-mail address: leonardo.pedrosa@tecnico.ulisboa.pt (L. Pedrosa).

interface with the setup is not made available; and (iii) all the parameters of the setup, except for the position of the three-way valves, are fixed, which restrains the universe of possible configurations. In this work, an original open-source design is proposed, which addresses these shortcomings. First, it is designed to be flexible, being possible to regulate several parameters to test different configurations. For instance, it is possible to: (i) select the position and direction of the zero of the process (see [3] for details); (ii) change the dimension of the cross-section and outlet holes of the tanks; (iii) add disturbance flows to all the tanks; (iv) implement either nonlinear control techniques or linear techniques using a linearization procedure; (v) study system identification techniques; and (vi) use either a single tank for single input single output (SISO) applications, at an introductory level of control education, or the whole setup for multiple input multiple output (MIMO) applications. Second, a user-friendly MATLAB/Simulink interface is developed, which supports a seamless shift between a numeric simulation of the quadruple-tank process dynamics and the interface with the physical experimental plant. This interface is achieved via USB serial communication with a personal computer running a custom Simulink block. It is important to mention that, although a MATLAB/Simulink interface is developed and provided, the control algorithms can be alternatively implemented directly in the Arduino microcontroller in C++ or in a personal computer, in any programming language, establishing a serial connection with the Arduino microcontroller. Third, all the materials and parts are inexpensive, can be readily obtained, and allow for a fast assembly. The CAD models of all the parts, the required technical drawings, the wiring schematics, the PCB design, the MATLAB/Simulink interface, assembly tutorials, and several examples are provided in the open-source repository available at <https://github.com/decenter2021/quadruple-tank-setup>. As a result, each setup is very easily reproducible, costs under 650€, and takes roughly 4 h to assemble.

There are commercial quadruple-tank setups for control education. It is true that the reproduction of the proposed apparatus requires ordering all the parts and manufacturing time by a technician with basic knowledge in electronics. However, in comparison, commercial solutions have several limitations. First, the acquisition cost is conservatively one order of magnitude higher than the cost of the setup presented in this paper, which is a prohibitive expense for many institutions. Second, maintenance is easier, since the setup is made of readily available low-cost parts. Third, since the whole design is open-source, some aspects of the design can be seamlessly adapted to specific needs, which is unattainable for a plug-and-play commercial solution. Fourth, the flexibility of the proposed design, which allows to test several configurations, cannot be matched by any commercial solution to the best of the authors' knowledge. In particular, when purchasing a commercial solution, the users are restricted to a specific acquisition board and corresponding interface, which constraints students, technicians, and researchers.

The outline of the paper is as follows. In Section 2, the quadruple-tank process experimental setup is described thoroughly regarding: (i) the process model; (ii) the design of the physical structure; (iii) the sensors, actuators, and their operation; and (iv) the interface with the experimental process via a personal computer. In Section 3, an identification procedure is proposed, which includes experimental results obtained with a prototype of the experimental setup. In Section 4, four control examples are presented with experimental results. Finally, Section 5 presents the main conclusions of this paper.

Throughout this paper, the identity and null matrices, both of appropriate dimensions, are denoted by \mathbf{I} and $\mathbf{0}$, respectively. Alternatively, \mathbf{I}_n and $\mathbf{0}_{n \times m}$ are also used to represent the $n \times n$ identity matrix and the $n \times m$ null matrix, respectively.

2. Description of the quadruple-tank process experimental setup

2.1. Process model

Consider four interconnected tanks as shown in Fig. 1. The water levels of tank 1 to tank 4 are denoted by h_1 , h_2 , h_3 , and h_4 . The network is controlled by two pumps, whose inputs are denoted by u_1 and u_2 , which are controlled by tank 1 and tank 2, respectively, in accordance with the schematic. Each pump is connected to a three-way valve that regulates the fraction of the flow, held constant, that goes to each of the tanks supplied by the pump. The fraction of flow of each pump that is directed to the lower tanks is denoted by γ_1 and γ_2 , respectively for tank 1 and tank 2. Each tank i has a cross section with an area A_i and the outlet hole has a cross section area a_i . Each tank has a sensor which measures its water level. Making use of mass balances and Bernoulli's law, the nominal system dynamics, in the absence of process noise and disturbances, are given by

$$\begin{cases} \dot{h}_1(t) = -\frac{a_1}{A_1} \sqrt{2gh_1(t)} + \frac{a_3}{A_1} \sqrt{2gh_3(t)} + \frac{\gamma_1 k_1}{A_1} u_1(t) \\ \dot{h}_2(t) = -\frac{a_2}{A_2} \sqrt{2gh_2(t)} + \frac{a_4}{A_2} \sqrt{2gh_4(t)} + \frac{\gamma_2 k_2}{A_2} u_2(t) \\ \dot{h}_3(t) = -\frac{a_3}{A_3} \sqrt{2gh_3(t)} + \frac{(1-\gamma_2)k_2}{A_3} u_2(t) \\ \dot{h}_4(t) = -\frac{a_4}{A_4} \sqrt{2gh_4(t)} + \frac{(1-\gamma_1)k_1}{A_4} u_1(t) \end{cases}, \quad (1)$$

where k_1 and k_2 are the constants of proportionality between the flow and the input for each pump, and g denotes the acceleration of gravity. Furthermore, the input of each pump is subject to a hard constraint $u_i \in [u_i^{\text{sat-}}, u_i^{\text{sat+}}]$, $i = 1, 2$. Additionally, one can also model disturbances as additive flows to the tanks. Thus, consider two additional pumps that can be used to provide disturbance flows when connected to any two of the four tanks, as illustrated in Fig. 1.

2.2. Physical setup design

The CAD model and physical implementation of the novel design proposed in this paper are presented in Fig. 2. It consists of a 1 m tall structure of 4 tanks supported by acrylic slabs. The water flows are directed using transparent flexible tubing. The water level is measured using one resistive water level sensor in each of the tanks. The valves, as well as several other components of the plant, are 3D printed. The setup is controlled via the circuit on the top slab of the plant with a dedicated PCB, which can be interfaced with MATLAB/Simulink via USB. The setup is powered with a 14 V DC transformer. An abridged parts list, with corresponding costs as of 2021, is presented in Table A.6 in Appendix. Each setup costs under 650€ and takes roughly 4 h to assemble. In this section, each of the components of the setup is described. The present paper aims to allow for an easy, fast, and low-cost reproduction of this setup. The full parts list, the CAD models of all the parts, the technical drawings of the acrylic slabs, the wiring schematic, the PCB design, the MATLAB/Simulink interface, and several examples are provided in the open-source repository available at <https://github.com/decenter2021/quadruple-tank-setup>.

2.2.1. Structure, tanks, valves, and tubing

This setup was carefully designed to be flexible, robust, low-cost, and very easily reproducible for various purposes. For that reason, it is designed to be regulable and to be able to test multiple configurations. It is possible to easily adjust the: (i) cross section of the outlet holes of all tanks, a_i ; (ii) cross section of all tanks, A_i ; and (iii) the fraction of flow that passes through the three-way valves to the lower tanks, γ_i . All the materials and

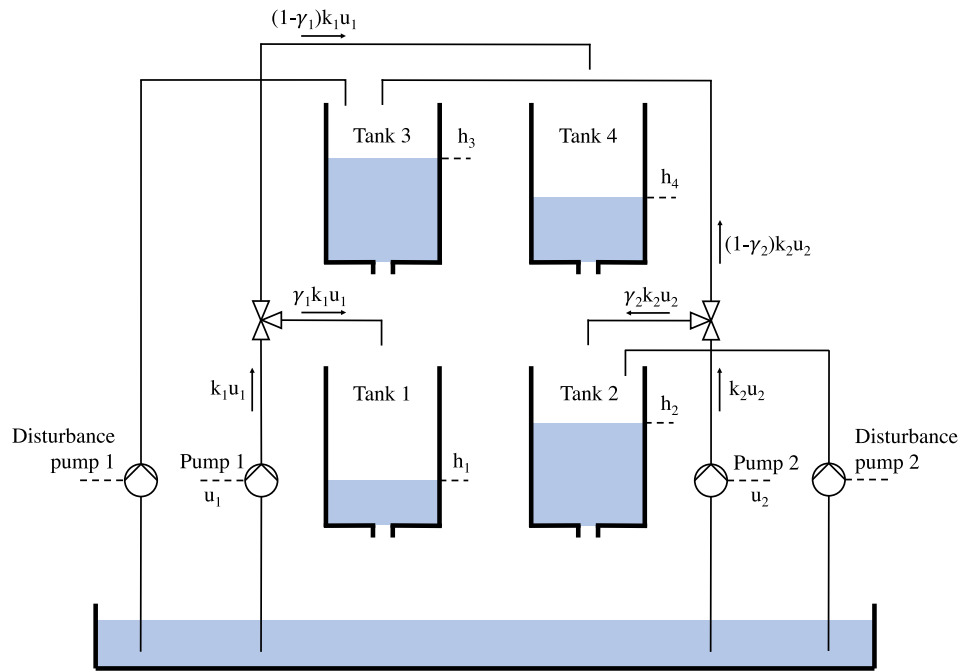
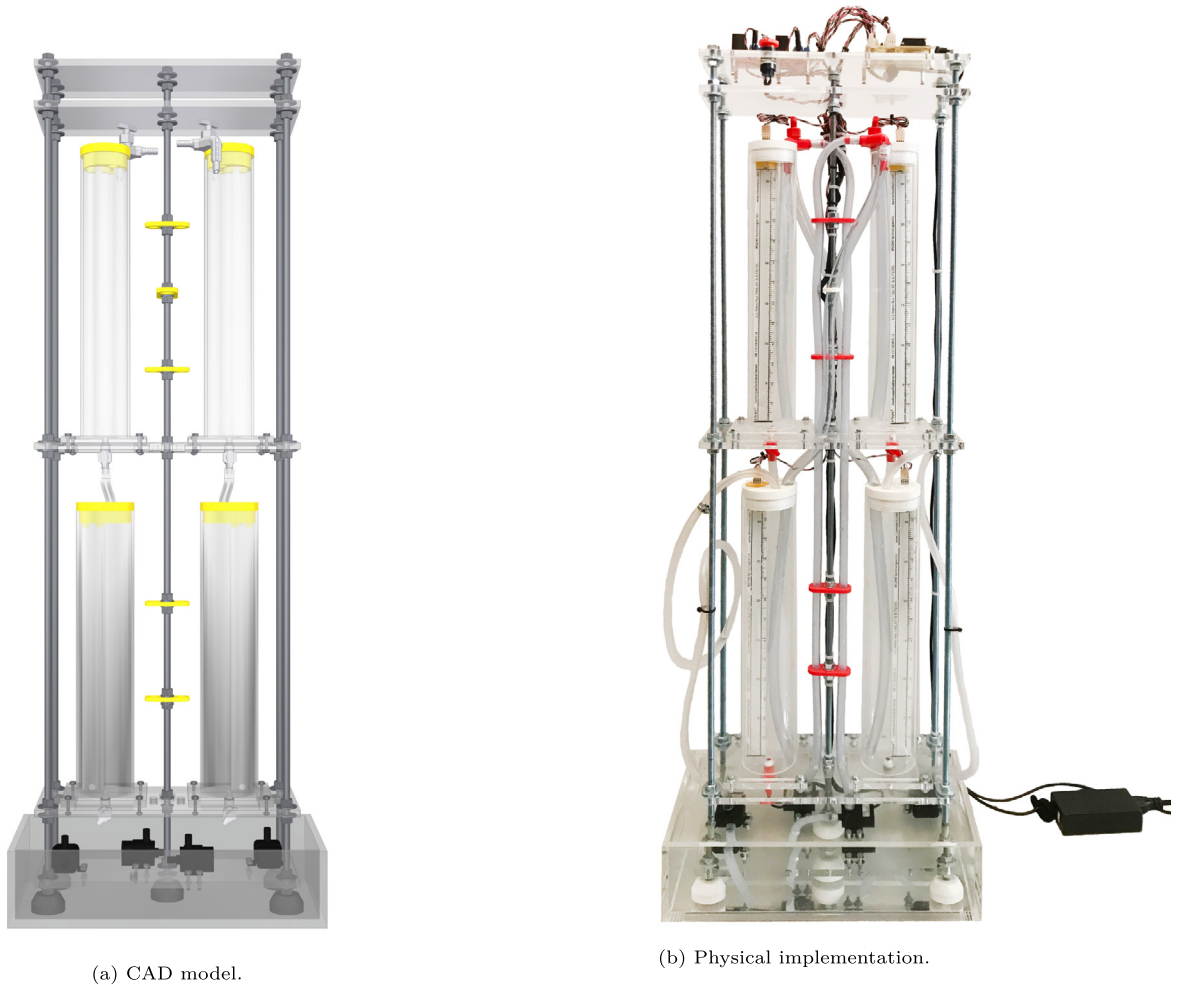


Fig. 1. Schematic of a quadruple-tank network with the illustrative addition of disturbance flows to tanks 2 and 3.



(a) CAD model.

(b) Physical implementation.

Fig. 2. Quadruple-tank process setup.

Table 1
Range of the physical parameters of the setup.

| Parameter | Range |
|------------------------|-----------------------------|
| $A_i, i = 1, \dots, 4$ | 22.90–84.95 cm ² |
| $a_i, i = 1, 2$ | 0–0.2376 cm ² |
| $\gamma_i, i = 1, 2$ | 0–1 |

parts are inexpensive, can be easily obtained, and allow for a fast assembly.

First, the backbone of the setup is constituted of acrylic parts. The slabs of acrylic are 8 mm thick and, together with structural fasteners, allow for a very sturdy structure. The water reservoir is not attached to the main setup, allowing for greater mobility. The technical drawings of these parts include the proper tolerances for fitting with the remaining parts and they are available at the aforementioned open-source repository. These technical drawings are suitable to be sent to an acrylic manufacturer. Although this structure is very stable, to ensure it does not tip over in case of an accident, the authors recommend that the two threaded rods on the back are secured with string and suction cups, for instance, to a vertical wall. The acrylic tanks are fastened to a slab using nuts and bolts. Therefore, it is very easy to switch a tank to test a different cross section, without having to rebuild the whole setup. The range of the cross section of the tanks is detailed in Table 1.

Second, there are also several 3D printed parts designed specifically for this purpose, which offer great flexibility, since they are cheap, readily printed, and easily adapted. The reader interested in reproducing the proposed setup may want to consider on-demand low-cost online 3D printing services, if the cost of acquiring a 3D printer is not worthy or if only a few setups are assembled. The CAD models of all the 3D printed parts are available in stl, 3mf, and also as editable Solid Edge part formats in the aforementioned open-source repository. The five threaded rod supports are 3D printed and designed to be fastened to the threads of the rods. Thus, it is possible to adjust each support with precision to balance the setup. Moreover, the outlet holes of all tanks are connected to 3D printed regulable valves, which allow to easily make modifications to the cross section of each outlet hole. The three-way valves are also 3D printed and allow for the fraction of flow that passes to the lower tanks to be regulable. The range of the value of the regulable parameters of the setup is presented in Table 1. Fig. 3 shows the coupling of the outlet valves of the upper tanks to the setup. A 3D render of the valve is presented in Fig. 4. A video tutorial of the assembly of a valve can be accessed at the aforementioned open-source repository.

Third, after careful design and experimentation, it was found that the best position for the three-way valves is above the upper tanks combined with the use of transparent flexible tubing with two different inner cross sections. In fact, to ensure that the fraction of flow that is diverted to the lower tanks by the three-way valve does not vary with the input flow, it is necessary that both outlets of the three-way valve are at the same static pressure. To achieve that, the outlet of the pump is connected to the inlet of the three-way valve, which divides the flow into two flexible tubes with a greater section area. The price to pay to ensure that γ_i does not vary with the flow of the i th pump with this configuration is the reduction of the maximum flow of the pump.

2.2.2. Electronics

First, the continuous fluid level sensor PN-12110215TC-12 was chosen to measure the water level in the tanks. It is sensitive to the hydrostatic pressure of the liquid it is immersed in, which

results in a change of the resistance of the sensor. It is connected in a simple voltage divider scheme, whose output V_0 is connected to a channel of a 16 bit analog-to-digital converter (ADC), which interfaces with the Arduino microcontroller using the Inter-Integrated Circuit (I2C) protocol. The computation of the water level from the ADC measurements and the calibration of the sensor are detailed in Section 3. These sensors are very accurate, but they are also very sensitive to physical perturbations and to bending, thus, they require an enclosure. Therefore, the sensors are fitted in a cylindrical acrylic tube with a 3D printed support that fits into the 3D printed caps of the tanks.

Second, the VMA421 water pump was chosen for this setup. The water flow of each pump can be controlled with the input voltage to the pump, up to 12 V DC. As described in Section 2.1, four pumps are used in this setup: (i) two for the actuation; and (ii) two additional pumps that can be used as disturbance water flows that can be connected to any two of the four tanks. The pumps are controlled using two L298N dual H-Bridge drivers using a pulse width modulation (PWM) signal for each pump. The pump characteristics are experimentally evaluated in Section 3. An emergency button is also added to disable the output of the driver to the pumps and stop them in case of an emergency.

Third, the whole setup is controlled via USB interfacing with an Arduino microcontroller that controls the pumps and reads the water level from the sensors. The plant is powered with a 14 V DC power supply. This allows for the maximum voltage available for the pumps, given that the MOSFETs on the drivers have a voltage drop of approximately 2 V. The Arduino is powered using a voltage regulator, to regulate the voltage of the power supply to 5 V DC. The electronic components of this setup are all connected via connectors to a PCB designed specifically for this purpose, which allows for an easy, fast, and clean setup. The wiring schematic of the setup is available at the aforementioned open-source repository, as well as the one layer design of the custom PCB. The schematic of the connection of the various electronic components to the PCB is presented in Fig. 5 and the connections on the real setup are shown in Fig. 6.

2.3. Setup interface with MATLAB/Simulink

The interface with the Arduino of the quadruple-tank process setup is done via USB with a custom Simulink block, which is shown in Fig. 7. This block, documentation, and supplementary files are available at the aforementioned open-source repository. It receives as input:

1. CLK, a clock signal, on whose rising edge the pump actuation is updated and a water level measurement is taken;
2. u (V), the 2×1 vector of the actuation signal which corresponds to the voltage input to the two actuation pumps;
3. d (PWM 8-bit), the 2×1 vector of the disturbance signal which corresponds to the PWM 8-bit values input to the two disturbance pumps;
4. ENB, which enables the 4 pumps if set to logical true and disables the 4 pumps if set to logical false.

And it outputs:

1. y_{gt} (cm), the 4×1 vector of the state signal, which corresponds to the ground truth water level in the four tanks;
2. y (cm), the 4×1 vector of the sensor measurement signal, which corresponds to the measured water level in the four tanks.

One key characteristic of this interface is that it allows for a seamless shift between a numeric simulation of the quadruple-tank process dynamics and the interface with the physical experimental plant. The selection of one of these modes is done by

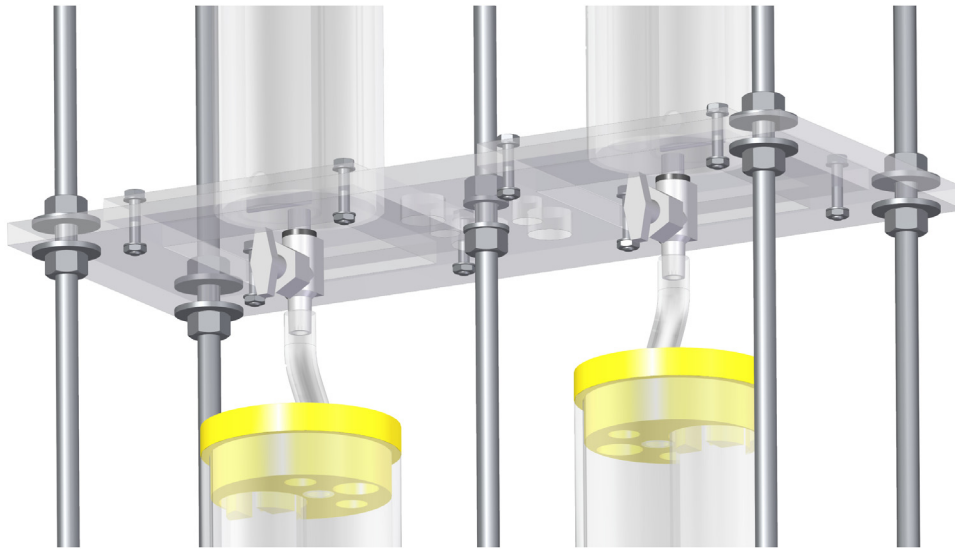
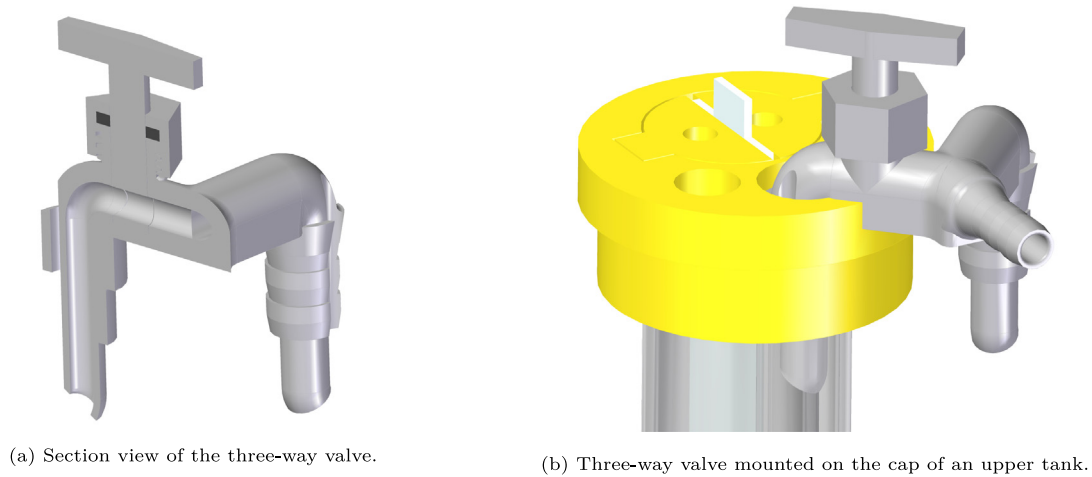


Fig. 3. Coupling of the outlet valves of the upper tanks to the setup.



(a) Section view of the three-way valve.

(b) Three-way valve mounted on the cap of an upper tank.

Fig. 4. Three-way valve.

defining the variable `experimentalSetup` on the active MATLAB workspace. It can be set to (i) logical true, to interface with the experimental setup in real time; or to (ii) logical false, to numerically simulate the dynamics of the quadruple-tank process; and (iii) if it is undefined, it defaults to the numerical simulation. It is strongly advised to numerically simulate a model before running it on the experimental setup. There are a few key differences between these two modes. On one hand, in the numerical simulation mode: (i) the simulated disturbances do not correspond accurately to the disturbances in the experimental plant, given that the experimental disturbance flow greatly depends on the position of the outlet. The magnitude of the simulated disturbance flows can be adjusted in the file `quadrupleLoadParameters.m`; (ii) the actuation pumps are always enabled no matter the input ENB; (iii) both process and sensor noise are modeled, according to

$$\begin{cases} \dot{h}_1(t) = -\frac{a_1}{A_1} \sqrt{2gh_1(t)} + \frac{a_3}{A_1} \sqrt{2gh_3(t)} + \frac{\gamma_1 k_1}{A_1} u_1(t) + w_1(t) \\ \dot{h}_2(t) = -\frac{a_2}{A_2} \sqrt{2gh_2(t)} + \frac{a_4}{A_2} \sqrt{2gh_4(t)} + \frac{\gamma_2 k_2}{A_2} u_2(t) + w_2(t) \\ \dot{h}_3(t) = -\frac{a_3}{A_3} \sqrt{2gh_3(t)} + \frac{(1-\gamma_2)k_2}{A_3} u_2(t) + w_3(t) \\ \dot{h}_4(t) = -\frac{a_4}{A_4} \sqrt{2gh_4(t)} + \frac{(1-\gamma_1)k_1}{A_4} u_1(t) + w_4(t) \\ y(t) = [h_1(t) \ h_2(t) \ h_3(t) \ h_4(t)]^T + \mathbf{v}(t) \end{cases},$$

where the vectors $\mathbf{w}(t) := [w_1(t) \ w_2(t) \ w_3(t) \ w_4(t)]^T$ and $\mathbf{v}(k)$ are the process and observation noise, modeled as zero-mean uncorrelated white Gaussian processes with associated covariance matrices $\mathbf{Q}_c(t) \succeq \mathbf{0} \in \mathbb{R}^{n \times n}$ and $\mathbf{R}_c(t) > \mathbf{0} \in \mathbb{R}^{o \times o}$, respectively, which are defined in the file `quadrupleLoadParameters.m`; and (iv) the ground truth output `y_gt` (cm) does not include sensor noise, whereas `y` (cm) includes sensor noise. On the other hand, in the experimental mode: (i) `y_gt` (cm) and `y` (cm) output the same value; (ii) the sensors are very accurate, thus additional noise can be added to `y` (cm) externally; and (iii) it is strongly advised to use blocks that support code generation in more complex models to reduce delays. The steps to create a new model to control the quadruple-tank experimental setup are detailed in the manual of the aforementioned repository. Various examples are provided therein as well, some of which are presented in Section 4.

The communication between the Arduino and the Simulink block is achieved using a full-duplex byte stream channel in a client-server configuration. The Arduino is the server in this configuration, which receives requests from the Simulink block of two types: (i) requests of the water level measurements; and (ii) requests of inputs to the pumps. All requests and responses are a byte stream block that follows the *binblock* protocol, the

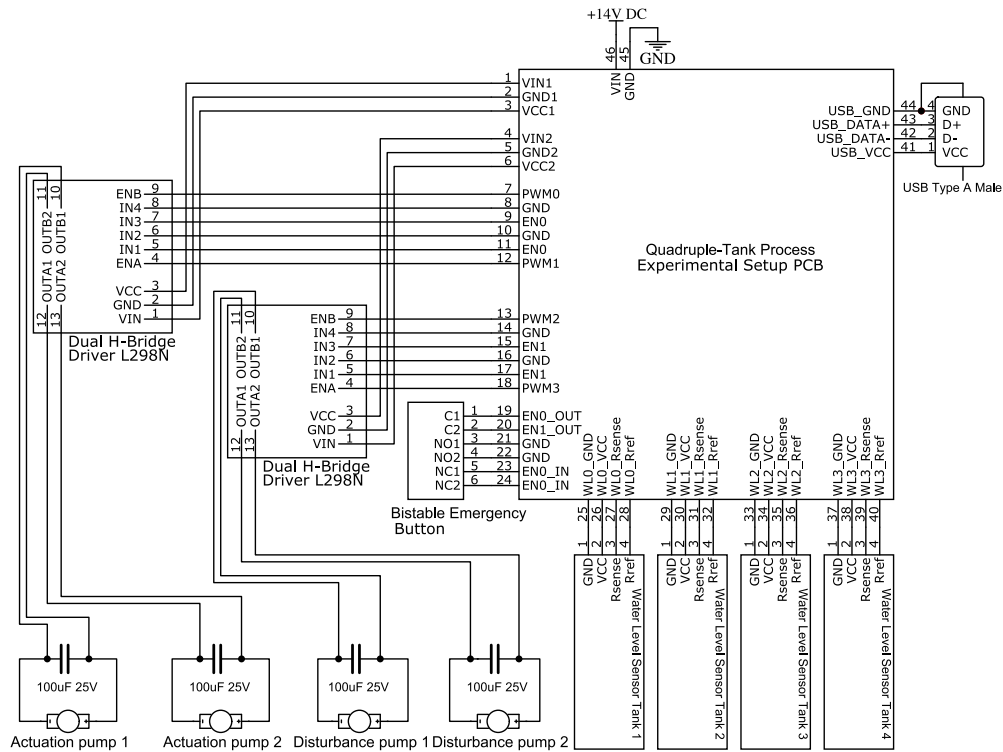


Fig. 5. Wiring schematic of the connection of the electrical components to the custom PCB.

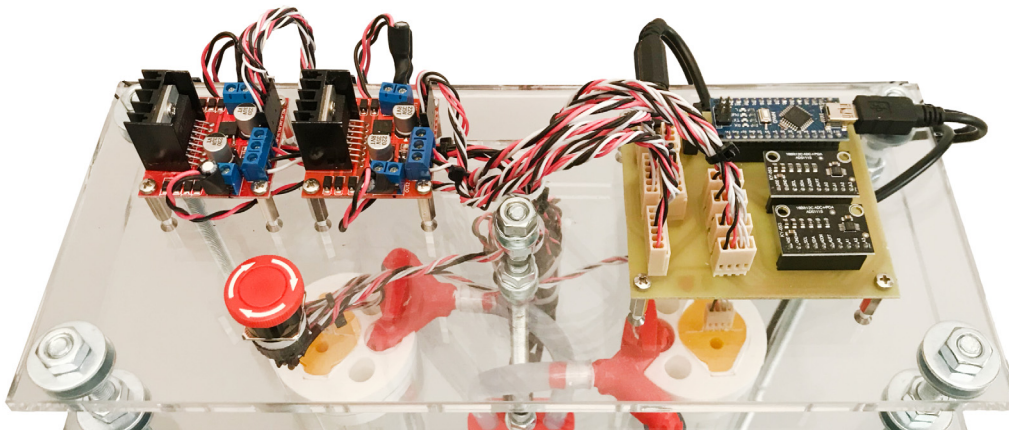


Fig. 6. Electronic components on the top of the setup.

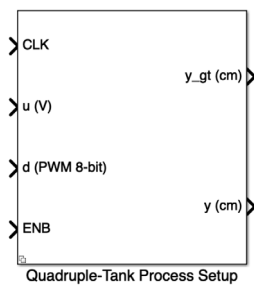


Fig. 7. Simulink block for interfacing with the quadruple-tank process experimental setup.

default protocol for serial communication with peripherals in MATLAB. If the Arduino does not receive any requests in a certain interval of time that can be defined, the pumps are disabled. More

details on the protocol and its implementation in the Arduino microcontroller are available and commented thoroughly at the aforementioned open-source repository.

3. Identification

In this section, a possible identification procedure is presented. This procedure consists of four steps, which can be carried out using a custom Simulink model and post-processing MATLAB scripts, all of which are made available and detailed thoroughly in the aforementioned open-source repository. Several .mat data files are generated in this procedure, some of which are required for the interface with the setup and may also be required for the synthesis procedure of a control law.

First, the section area of each tank is determined, whose proposed procedure is detailed in the aforementioned repository. Second, the characteristic slope of the water level sensors is determined. The water level sensor is made of two resistors: a

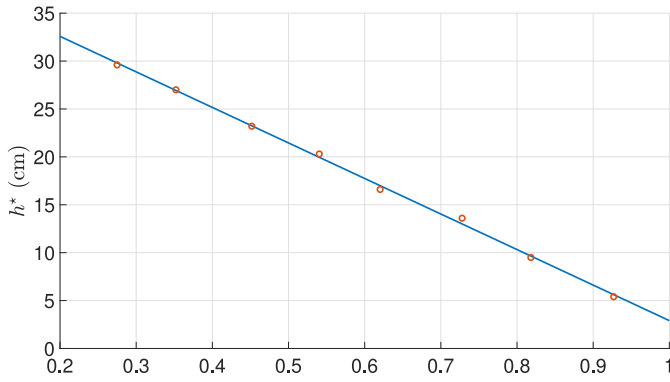


Fig. 8. Linear regression of illustrative experimental measurements taken for the water level sensor in tank 1.

reference resistor, R_{ref} , and a resistor sensible to water level, R_{sense} . The sensor is connected in a simple voltage divider configuration, which outputs the voltage across the reference resistor, V_{ref} . Thus, $V_{ref}/V_{cc} = R_{ref}/(R_{ref} + R_{sense})$. The ratio $r = R_{sense}/R_{ref}$ is known to be proportional to water level, i.e.,

$$h = (dh/dr)r + h_0. \quad (2)$$

It is important to point out that h_0 and h are measured relatively to the valve outlet hole, not the bottom of the tank or the zero of the sensor ruler. Gathering data points (r, h^*) , where h^* denotes water level measurements performed on the sensor ruler, according to the procedure described in the repository, an estimate of dh/dr can be obtained performing a linear regression. Fig. 8 shows a linear regression of illustrative experimental measurements taken for the water level sensor in tank 1. Note that the value of h_0 is still unknown, and it is only identified in the fourth step.

Third, the response of the pumps and the parameter γ of the three-way valves are identified. The pumps are controlled with a PWM signal, which is input to the pump driver. However, it can be experimentally verified that the evolution of the water flow through the pump with the width of the PWM signal is nonlinear. Nevertheless, to achieve linear control input dynamics, as presented in the model of the quadruple-tank process, one can consider instead a virtual input u , such that the water flow of the pump, q , is given by the linear relation $q = ku$, where k is a real number. Thus, the virtual input u ought to be a nonlinear function of the width of the PWM signal. Furthermore, saturation limits $[u^{sat-}, u^{sat+}]$ for the virtual control input can be defined to model the operation limits of the pump. It is experimentally verified that the curve $u(\text{PWM})$ can be approximated by

$$u(\text{PWM}) = c_1 \frac{\text{PWM} - c_3}{\text{PWM} - c_2}, \quad (3)$$

where PWM is the width of the PWM input normalized to the range $[0, 1]$, and c_1 , c_2 , and c_3 are real constants. After these constants have been identified, one can freely set the upper saturation limit u^{sat+} , thus, the parameter k is given by

$$k = q_{\max}/u^{sat+} = \frac{c_1(1 - c_3)}{u^{sat+}(1 - c_2)},$$

where q_{\max} denotes the maximum flow which corresponds to $\text{PWM} = 1$. Moreover, inverting the transformation (3), for a desired input voltage to the pumps u , the PWM value that should be input is given by

$$\text{PWM} = \frac{c_1 c_3 - c_2 k u}{c_1 - k u}.$$

Table 2

Experimentally identified parameters of the first, second, and fourth steps of the proposed procedure.

| Parameter | Tank 1 | Tank 2 | Tank 3 | Tank 4 |
|-----------|------------------------|------------------------|-------------------------|-------------------------|
| A | 29.79 cm ² | 29.79 cm ² | 20.74 cm ² | 20.49 cm ² |
| dh/dr | -37.09 cm | -35.33 cm | -34.83 cm | -34.38 cm |
| a | 0.1241 cm ² | 0.1350 cm ² | 0.03327 cm ² | 0.03310 cm ² |
| h_0 | 43.42 cm | 41.13 cm | 46.99 cm | 39.35 cm |

Table 3

Experimentally identified parameters of the third step of the proposed procedure.

| Parameter | Pump 1 | Pump 2 |
|------------|---|---|
| u^{sat-} | 0 V | 0 V |
| u^{sat+} | 12 V | 12 V |
| c_1 | 39.01 cm ³ s ⁻¹ | 41.15 cm ³ s ⁻¹ |
| c_2 | -1.214 × 10 ⁻³ | 9.874 × 10 ⁻³ |
| c_3 | 33.86 × 10 ⁻³ | 43.04 × 10 ⁻³ |
| k | 3.137 cm ³ s ⁻¹ V ⁻¹ | 3.314 cm ³ s ⁻¹ V ⁻¹ |
| γ | 0.7569 | 0.7563 |

Gathering data points (q, γ, PWM) , according to the procedure proposed in the repository, it is possible to estimate c_1 , c_2 , c_3 , and k from a nonlinear least squares regression, for instance, of model (3). Fig. 9(a) shows illustrative experimental data and a nonlinear least squares fit to the model (3). Fig. 9(b) shows the experimental variation of the parameter γ_1 with the flow of pump 1. It is possible to confirm that the position of the valves successfully achieves an approximately constant value of γ .

Fourth, the outlet section area a and height datum h_0 of the tanks are determined. Consider a single tank and assume that it does not receive water from any other tanks. Note that it is possible to obtain this configuration in practice for all tanks, if only one of the actuation pumps is activated. In these conditions, from (1), in steady-state the water level of a lower tank satisfies

$$a\sqrt{2gh} = \gamma ku. \quad (4)$$

An analogous expression can be written for the upper tanks. Again, note that h_0 and h are measured relatively to the valve outlet hole, not the bottom of the tank or the zero of the sensor ruler. Writing (4) with respect to h and substituting it in the sensor model (2), one can write

$$r = \frac{\gamma^2 k^2}{2g a^2 (dh/dr)} u^2 - \frac{h_0}{dh/dr}. \quad (5)$$

Note that, according to (5), the dependence between r and u^2 is linear, thus, one can write $r = \alpha u^2 + \beta$, where the scalar constants α and β satisfy

$$a = \gamma k \frac{1}{\sqrt{2g\alpha(dh/dr)}} \quad \text{and} \quad h_0 = -\beta(dh/dr). \quad (6)$$

Gathering data points (r, u^2) in steady-state, according to the procedure proposed in the repository, it is possible to estimate α and β from a linear regression. Then, a and h_0 can be determined making use of (6). Fig. 10 shows the linear regression of illustrative experimental measurements of tank 1. It is possible to confirm that the model of the water outflow is accurate, since there is an approximately linear trend in this plot. Tables 2 and 3 present the experimental identification parameters for a configuration of the network, which is the same for the examples presented in Section 4.

4. Application examples

In this section, four control-theory examples are presented. In all these examples, the parameters of the setup are those detailed

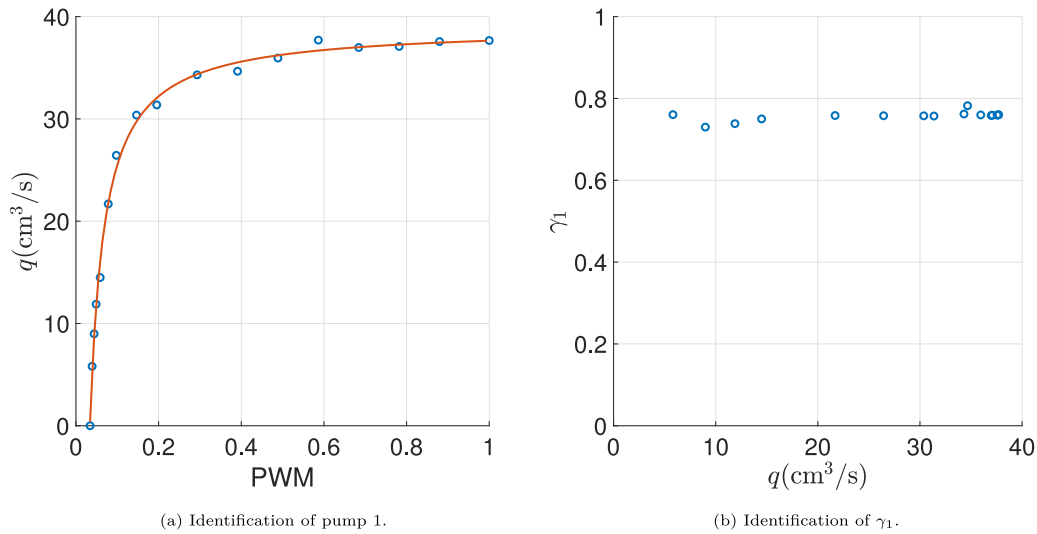


Fig. 9. Illustrative experimental measurements of the third step of the identification procedure.

Table 4 Learning outcomes associated with each application example.

| Example | Illustrative learning outcomes |
|---|---|
| PI control of a single tank (Section 4.1) | (i) linearization; (ii) state-feedback; (iii) pole placement (e.g. root locus); (iv) P, PI, and PID controllers; (v) Ziegler–Nichols tuning procedure; (vi) reference tracking; and (vii) disturbance rejection |
| Frequency response of a single tank (Section 4.2) | (i) linearization; (ii) frequency response; (iii) loop shaping; and (iv) identification based on frequency response |
| Quadruple-tank reference tracking (Section 4.3) | (i) linearization; (ii) state-space control; (iii) effect of the position and direction of zeros; (iv) anti wind-up techniques; and (v) nonlinear control techniques |
| Decentralized reference tracking (Section 4.4) | Validation of state-of-the-art control solutions |

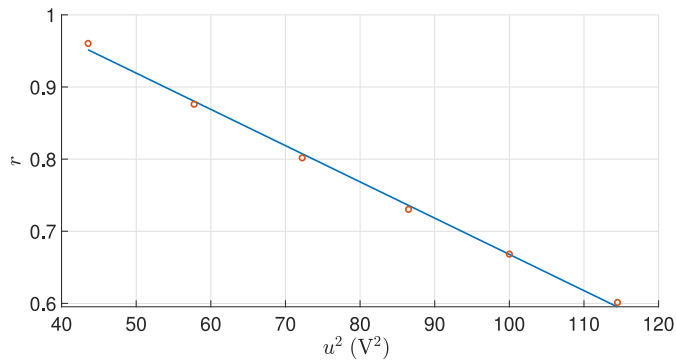


Fig. 10. Linear regression of illustrative experimental measurements taken to determine the outlet section area a and height datum h_0 of tank 1.

in Tables 2 and 3. All the models, supplementary scripts, raw experimental data of each example, and videos of the experimental simulations are available at the aforementioned open-source repository. Some of the possible learning outcomes associated with each example are listed in Table 4.

4.1. Proportional–integral control of a single tank

The application of a proportional–integral (PI) controller to track a reference water level of a single tank is addressed first. The Simulink model is presented in Fig. 11. Note that it is very easy to design a feedback loop in the interface block and the shift between numerical and experimental modes only requires the change of a workspace variable. The PI gains were adjusted

empirically and a simple anti wind-up scheme was also employed to saturate the integral state. An impulsive disturbance is considered at $t = 300$ s and a constant disturbance starting at $t = 450$ s until the end of the simulation. The output, as well as the control action, are presented in Fig. 12 for a numeric simulation and experimental results. The evolution of the numeric and experimental results is very similar. It is also possible to see that the water level sensors are very accurate and that the experimental setup was able to rapidly react to impulsive and constant disturbances.

4.2. Frequency response of a single tank

The frequency response of a single tank is also an interesting application. Given that the dynamics of the process are nonlinear, the frequency analysis is carried out about an equilibrium point. From the nonlinear dynamics of the quadruple-tank process (1), the dynamics for tank 1 can be linearized about an equilibrium operation water level \bar{h}_1 and actuation \bar{u}_1 . Taking the Laplace Transform of the linearized dynamics with a null initial condition yields

$$\frac{\Delta h_1(s)}{\Delta u_1(s)} = \frac{\gamma_1 k_1 / A_1}{s + \frac{a_1}{A_1} \sqrt{\frac{g}{2h_1}}}, \tag{7}$$

where $\Delta h_1(t) := h_1(t) - \bar{h}_1$ and $\Delta u_1(t) := u_1(t) - \bar{u}_1$. For $\bar{u}_1 = 8$ V, pairs (A_i, A_o) were measured for various values of frequency. Fig. 13 shows the evolution of the gain, i.e., the ratio A_o/A_i , with the frequency of the input signal. The horizontal line represents the value of the DC gain. From Fig. 13, it appears that the experimental results converge to the expected high frequency asymptotic linear evolution, in the logarithmic scale, for $f \geq$

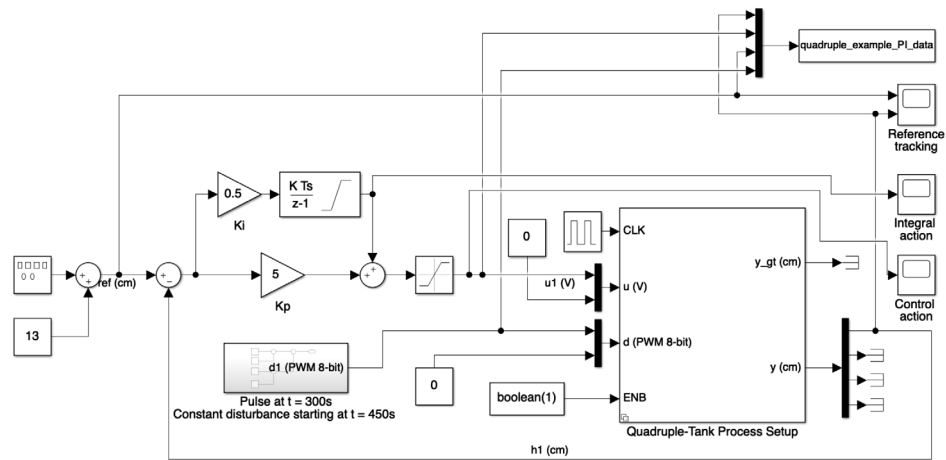
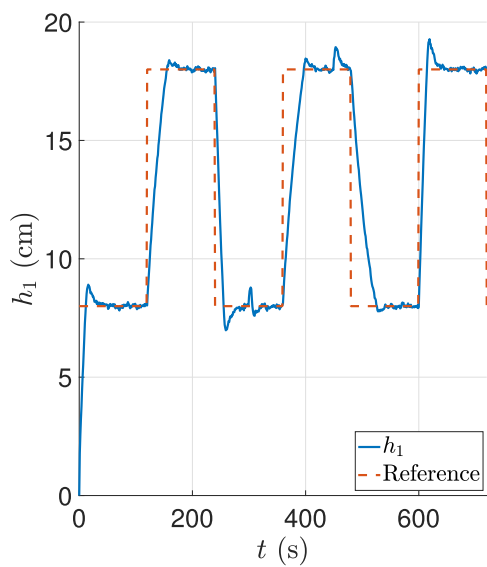
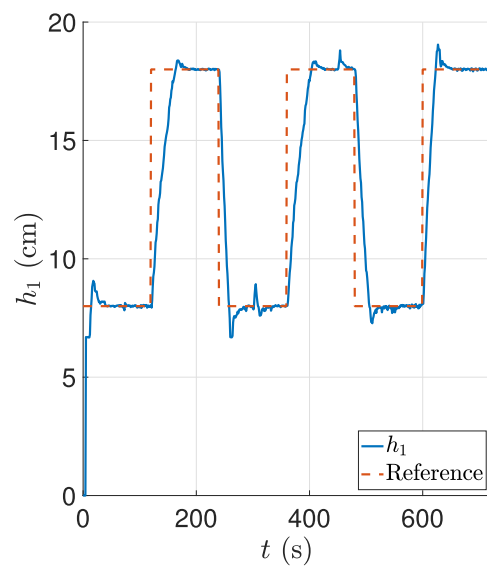


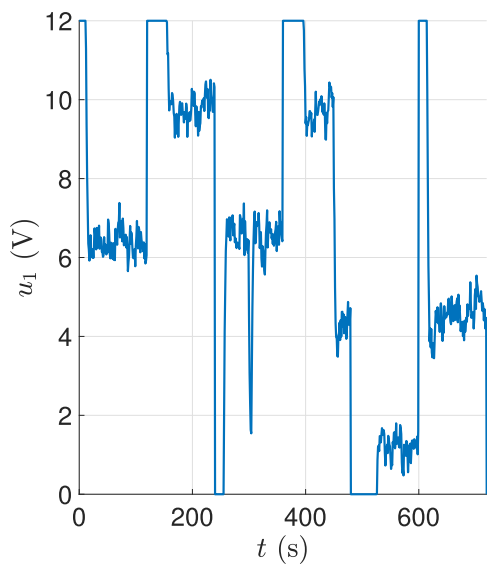
Fig. 11. Simulink model of a PI controller to track a reference water level of a single tank.



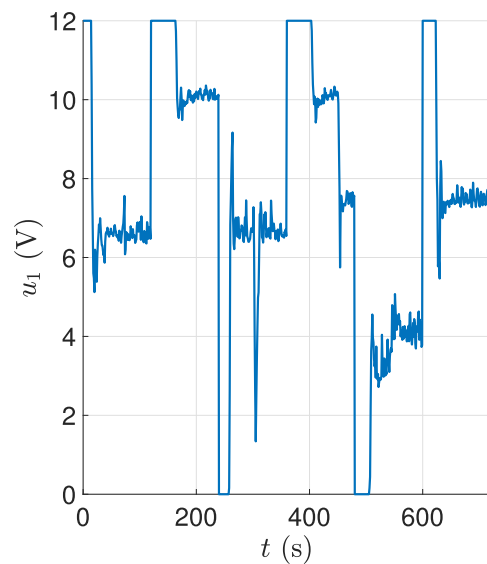
(a) Numerical results: evolution of h_1 .



(b) Experimental results: evolution of h_1 .



(c) Numerical results: evolution of u_1 .



(d) Experimental results: evolution of u_1 .

Fig. 12. Evolution of the output and control action of the quadruple-tank process PI controller for both numerical simulations and experimental results.

Table 5
Comparison of frequency response parameters obtained with simulations and their theoretical value.

| Parameter | Theoretical value | Estimated numerically | Estimated experimentally |
|------------------|-----------------------------|-----------------------------|-----------------------------|
| DC gain | 3.214 cm V ⁻¹ | 3.320 cm V ⁻¹ | 2.660 cm V ⁻¹ |
| Pole | 0.0248 rad s ⁻¹ | 0.0224 rad s ⁻¹ | 0.0331 rad s ⁻¹ |
| Regression slope | -20.00 dB dec ⁻¹ | -19.60 dB dec ⁻¹ | -20.81 dB dec ⁻¹ |

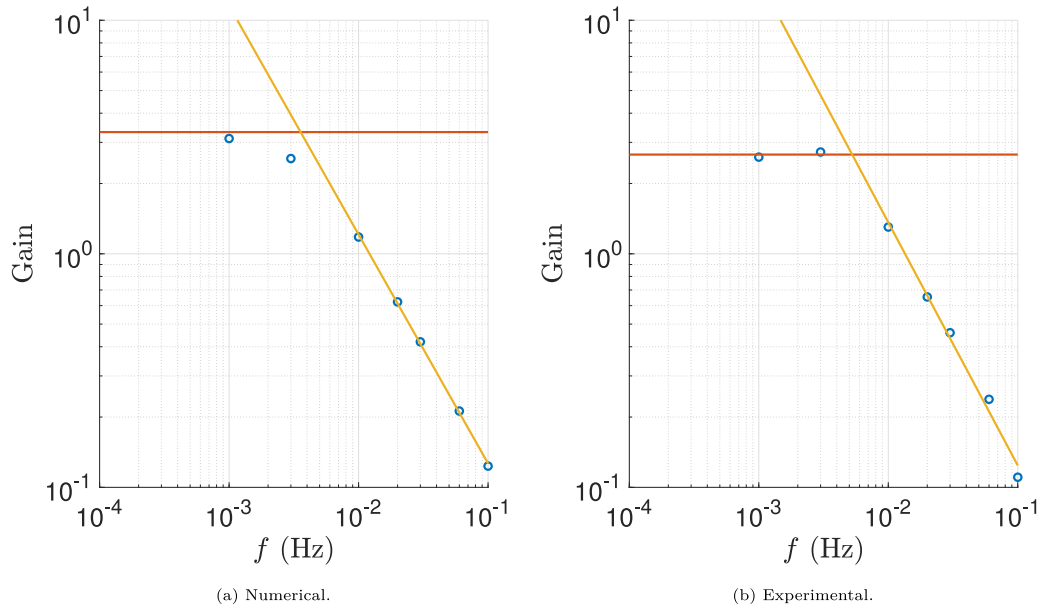


Fig. 13. Evolution of the gain with frequency for tank 1.

10^{-2} Hz. A linear regression of the data points with $f \geq 10^{-2}$ Hz, in the logarithmic scale, is also represented in the plots. Table 5 presents the estimated frequency response parameters and their theoretical value, obtained from (7). The pole is approximated, using numeric and experimental data, by the frequency at which the asymptotic regression reaches the DC gain. The results show that the experimentally obtained parameters are close to the corresponding theoretical values and, thus, this is also an adequate identification procedure.

4.3. Quadruple-tank process reference tracking

In this section, a simple linear quadratic regulator (LQR) [23] is synthesized to track a reference water level in the lower tanks. The nonlinear dynamics (1) can be linearized about a given equilibrium point, characterized by equilibrium water levels $h_1^0, h_2^0, h_3^0, h_4^0$; and inputs u_1^0, u_2^0 . The linearized continuous-time system can be discretized with a sampling period T , yielding a discrete-time system of the form

$$\mathbf{x}(k+1) = \mathbf{A}\mathbf{x}(k) + \mathbf{B}\mathbf{u}(k),$$

where $\mathbf{x}(k) := [h_1(k) - h_1^0 \quad \dots \quad h_4(k) - h_4^0]^T$ and $\mathbf{u}(k) := [u_1(k) - u_1^0 \quad u_2(k) - u_2^0]^T$. To add robustness to the tracker, consider new state variables that correspond to the integral of the tracking error, given by

$$\mathbf{x}_I(k) = \sum_{\tau=0}^{k-1} (\mathbf{H}\mathbf{x}(\tau) - \mathbf{r}(\tau)),$$

where $\mathbf{r}(\tau) \in \mathbb{R}^{2 \times 1}$ is the reference water level signal for the lower tanks, and \mathbf{H} is the output tracking matrix, given by $\mathbf{H} = [\mathbf{I}_2 \quad \mathbf{0}_{2 \times 2}]$ to track a reference with the water level of the lower tanks. Then, one can define the augmented system

$$\begin{bmatrix} \mathbf{x}(k+1) \\ \mathbf{x}_I(k+1) \end{bmatrix} = \begin{bmatrix} \mathbf{A} & \mathbf{0} \\ \mathbf{H} & \mathbf{I} \end{bmatrix} \begin{bmatrix} \mathbf{x}(k) \\ \mathbf{x}_I(k) \end{bmatrix} + \begin{bmatrix} \mathbf{B} \\ \mathbf{0}_{2 \times 2} \end{bmatrix} \mathbf{u}(k) + \begin{bmatrix} \mathbf{0}_{4 \times 2} \\ -\mathbf{I}_2 \end{bmatrix} \mathbf{r}(k). \quad (8)$$

One can, now, add the integral action feedback term applying a LQR to the augmented system (8) with state and input weighting matrices \mathcal{Q} and \mathcal{R} , respectively, to obtain an augmented gain $\mathcal{K} = [\mathbf{K} \quad \mathbf{K}_I]$. Furthermore, to improve the transient response, one can also include a feedforward term, yielding a control action of the form

$$\mathbf{u}(k) = \mathbf{u}^0 - \mathcal{K}(\mathbf{x}(k) - \mathbf{x}^0) - \mathbf{K}_I \mathbf{x}_I(k) + \mathbf{N}\mathbf{r}(k),$$

where $\mathbf{x}^0 := [h_1^0 \quad h_2^0 \quad h_2^0 \quad h_4^0]^T$, $\mathbf{u}^0 := [u_1^0 \quad u_2^0]^T$, and $\mathbf{N} \in \mathbb{R}^{2 \times 2}$ is computed such that the DC gain of the closed-loop system without integral action is unitary, i.e., $\mathbf{N} = (\mathbf{H}(\mathbf{I} - \mathbf{A} + \mathbf{B}\mathbf{K})^{-1}\mathbf{B})^{-1}$.

This controller is synthesized for an equilibrium point characterized by $h_1^0 = h_2^0 = 14$ cm. Impulsive and constant disturbances are felt starting at $t = 300$ s until the end of the simulation. A simple anti wind-up scheme was also employed to saturate the integral states. More details on the gain synthesis and Simulink model can be found at the aforementioned open-source repository. The output, as well as the control action, are depicted in Fig. 14 for a numeric simulation and an experimental result. The evolution of the numeric and experimental results is very similar except for tank 3, which suggests a poorer identification for this tank. It is also possible to see that the synthesized control law is able to successfully track a reference signal and to reject impulsive and constant disturbances.

4.4. Quadruple-tank process decentralized reference tracking

In this section, the state-of-the-art decentralized tracker put forward in [24] for linear time-varying (LTV) systems is experimentally applied to the quadruple-tank process experimental setup. Similarly to the centralized tracker presented in Section 4.3, to employ this decentralized strategy, the process dynamics are approximated by a LTV system, linearizing and discretizing its dynamics about successive equilibrium points. Impulsive and constant disturbances are felt starting at $t = 300$ s

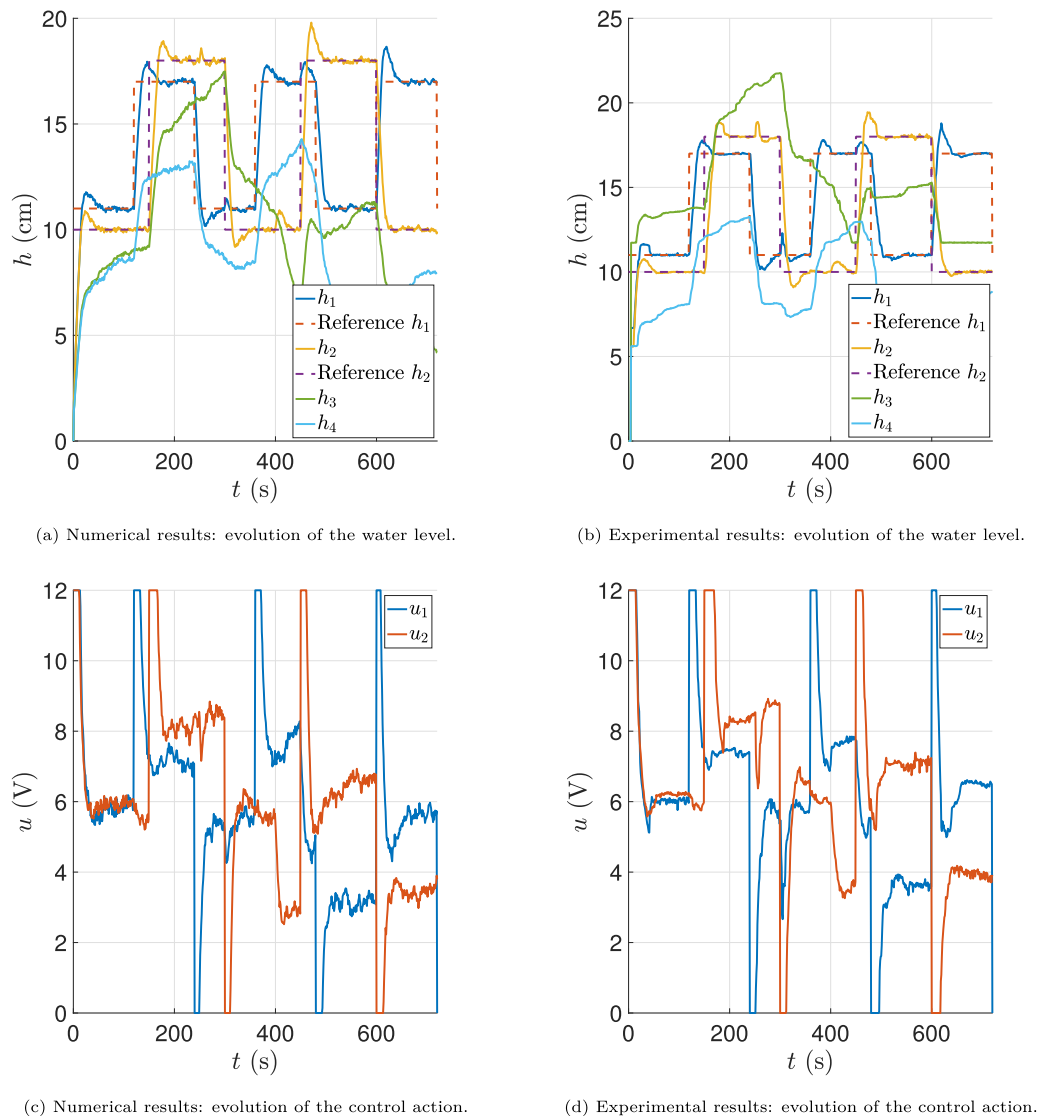


Fig. 14. Evolution of the output and control action of the quadruple-tank process LQR controller for both numerical simulations and experimental results.

until the end of the simulation. The output, as well as the control action, are presented in Fig. 15 for a numeric simulation and an experimental result. Again, the evolution of the numeric and experimental results is very similar except for tank 3, which suggests a poorer identification for this tank. It is also possible to see that the synthesized decentralized control law is able to successfully track a time-varying reference signal and to reject impulsive and constant disturbances.

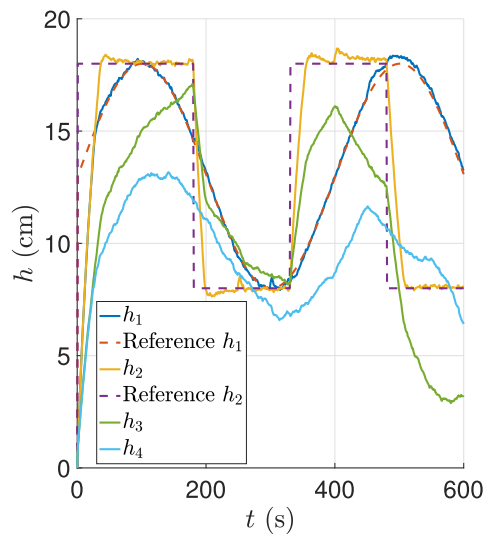
5. Conclusion

The major hurdle in accessing laboratory experimentation is the cost of acquiring experimental scientific equipment, which is unbearable for many institutions that struggle for funding. In this paper, an apparatus of four interconnected tanks is designed to be low-cost, flexible, easily reproducible, and fast to assemble. All data, files, and software necessary to reproduce this apparatus are provided in an open-access repository. The setup costs under 650€ and takes roughly 4 h to assemble. An illustrative experimental identification of the setup allowed to validate the proposed design and confirm that it is in accordance with the nominal process dynamics. Several application examples were detailed to illustrate the flexibility of the setup, not only

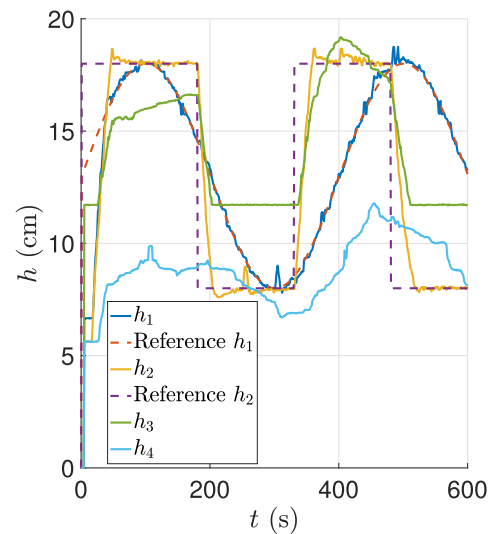
for control education, but also for the validation of state-of-the-art techniques. The proposed setup is suitable for control instruction in several topics such as: (i) system identification; (ii) linearization; (iii) frequency/time response; (iv) state feedback (e.g. root locus); (v) P, PI, and PID controllers; (vi) Ziegler–Nichols tuning procedure; (vii) disturbance rejection; (viii) state-space control (e.g. LQR); (ix) effect of the position and direction of zeros (e.g. non-minimum phase zeros); (x) nonlinear control; and (xi) decentralized control. Finally, the readers that are interested in reproducing this experimental setup are invited to contribute with application examples and suggest improvements.

CRediT authorship contribution statement

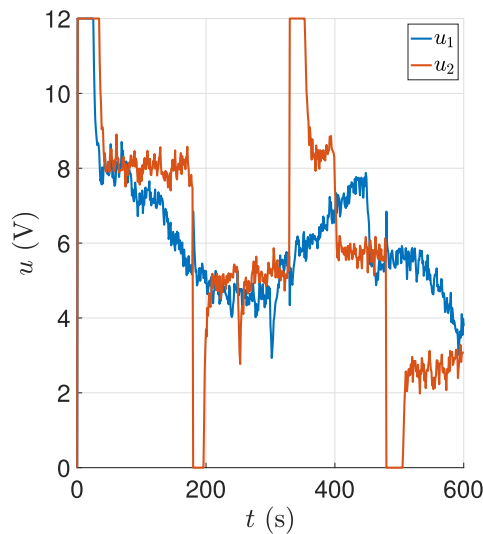
Leonardo Pedroso: Conceptualization, Data curation, Formal analysis, Investigation, Methodology, Resources, Software, Validation, Visualization, Writing – original draft, Writing – review & editing. **Pedro Batista:** Conceptualization, Funding acquisition, Methodology, Project administration, Resources, Supervision, Validation, Visualization, Writing – review & editing.



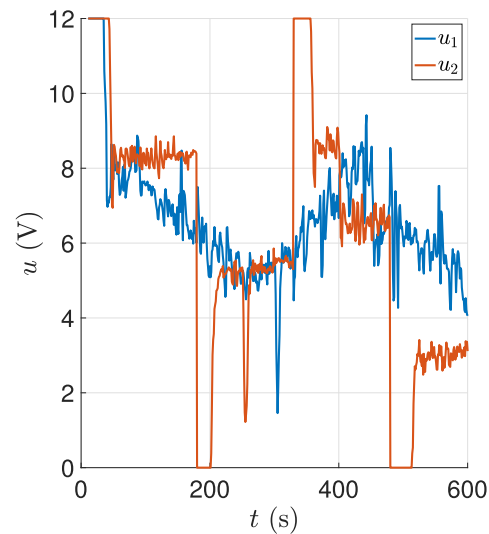
(a) Numerical results: evolution of the water level.



(b) Experimental results: evolution of the water level.



(c) Numerical results: evolution of the control action.



(d) Experimental results: evolution of the control action.

Fig. 15. Evolution of the output and control action of the quadruple-tank process decentralized tracker for both numerical simulations and experimental results.

Declaration of competing interest

The authors declare that they have no known competing financial interests or personal relationships that could have appeared to influence the work reported in this paper.

Data availability

The data that support the findings of this study are openly available at <https://github.com/decenter2021/quadruple-tank-setup>.

Acknowledgments

This work was supported by the Fundação para a Ciência e a Tecnologia (FCT), Portugal through LARSyS - FCT Project UIDB/50009/2020 and through the FCT project DECENTER [LISBOA-01-0145-FEDER-029605], funded by the Programa Operacional Regional de Lisboa 2020 and PIDDAC programs, Portugal.

Appendix. Parts list

Table A.6
Quadruple-tank setup abridged parts list.

| Part | Cost |
|---|-------------|
| Acrylic parts | 223€ |
| Structural parts | 54.5€ |
| 3D printed parts | 12.5€ |
| Connectors | 37.5€ |
| Arduino Nano | 7€ |
| 4x Continuous fluid level sensor PN-12110215TC-12 | 136€ |
| 4x VMA421 water pump | 72€ |
| 2x L298N Dual H-Bridge Driver | 9€ |
| 2x ADS 1115 ADC | 20€ |
| 14VDC 2.5 A 35 W power supply | 21€ |
| Bi-stable emergency button | 12€ |
| Custom PCB with connectors | 35€ |
| Miscellaneous electronics parts | 3.5€ |
| Total | 643€ |

References

[1] R. Grepl, Real-time control prototyping in MATLAB/Simulink: review

- of tools for research and education in mechatronics, in: 2011 IEEE International Conference on Mechatronics, IEEE, 2011, pp. 881–886.
- [2] P. Menghal, A.J. Laxmi, Real time simulation: A novel approach in engineering education, in: 2011 3rd International Conference on Electronics Computer Technology, Vol. 1, IEEE, 2011, pp. 215–219.
- [3] K. Johansson, The quadruple-tank process: a multivariable laboratory process with an adjustable zero, *IEEE Trans. Control Syst. Technol.* 8 (3) (2000) 456–465, <http://dx.doi.org/10.1109/87.845876>.
- [4] R. Saco, E. Pires, C. Godfrid, Real time controlled laboratory plant for control education, in: 32nd Annual Frontiers in Education, Vol. 1, IEEE, 2002, <http://dx.doi.org/10.1109/FIE.2002.1157934>.
- [5] P.S. Shiakolas, D. Piyabongkarn, Development of a real-time digital control system with a hardware-in-the-loop magnetic levitation device for reinforcement of controls education, *IEEE Trans. Educ.* 46 (1) (2003) 79–87.
- [6] P. de Moura Oliveira, J.D. Hedengren, J. Rossiter, Introducing digital controllers to undergraduate students using the tclab arduino kit, *IFAC-PapersOnLine* 53 (2) (2020) 17524–17529.
- [7] M.K. Bayrakceken, A. Arisoy, An educational setup for nonlinear control systems: Enhancing the motivation and learning in a targeted curriculum by experimental practices [focus on education], *IEEE Control Syst. Mag.* 33 (2) (2013) 64–81.
- [8] J. Rossiter, S. Pope, B.L. Jones, J. Hedengren, Evaluation and demonstration of take home laboratory kit, *IFAC-PapersOnLine* 52 (9) (2019) 56–61.
- [9] P.M. Oliveira, J.D. Hedengren, An apmonitor temperature lab PID control experiment for undergraduate students, in: 2019 24th IEEE International Conference on Emerging Technologies and Factory Automation (ETFA), IEEE, 2019, pp. 790–797.
- [10] J. Park, R.A. Martin, J.D. Kelly, J.D. Hedengren, Benchmark temperature microcontroller for process dynamics and control, *Comput. Chem. Eng.* 135 (2020) 106736.
- [11] R. Dormido, H. Vargas, N. Duro, J. Sánchez, S. Dormido-Canto, G. Farias, F. Esquembre, S. Dormido, Development of a web-based control laboratory for automation technicians: The three-tank system, *IEEE Trans. Educ.* 51 (1) (2008) 35–44.
- [12] J. Sotomayor-Moriano, G. Pérez-Zúñiga, M. Soto, A virtual laboratory environment for control design of a multivariable process, *IFAC-PapersOnLine* 52 (9) (2019) 15–20.
- [13] T. Scott, Versatile, low cost external convective heat transfer apparatus, in: 2004 Annual Conference, No. 10.18260/1-2–13626, ASEE Conferences, Salt Lake City, Utah, 2004, <https://peer.asee.org/13626>.
- [14] N.B. Pour, D.B. Thiessen, R.F. Richards, B.J. Van Wie, Improving student understanding and motivation in learning heat transfer by visualizing thermal boundary layers, *Int. J. Eng. Educ.* 33 (2A) (2017) 723–740.
- [15] N.B. Pour, D.B. Thiessen, B.J. Van Wie, Improving student understanding and motivation in learning heat transfer by visualizing thermal boundary layers, *Int. J. Eng. Educ.* 34 (2A) (2018) 514–526.
- [16] A. Howell, R. Eckert, R. McGrann, Results of using a low cost, flexible robot in a microcontrollers and robotics course, in: 2008 Annual Conference & Exposition, No. 10.18260/1-2–3138, ASEE Conferences, Pittsburgh, Pennsylvania, 2008.
- [17] R.W. Krauss, C.T. VanderRoest, Board # 144 : MAKER: A 3D printed balancing robot for teaching dynamic systems and control, in: 2017 ASEE Annual Conference & Exposition, No. 10.18260/1-2–27760, ASEE Conferences, Columbus, Ohio, 2017.
- [18] R.W. Krauss, Combining course flipping and a low-cost experiment to teach frequency response, in: 2018 ASEE Annual Conference & Exposition, No. 10.18260/1-2–30202, ASEE Conferences, Salt Lake City, Utah, 2018.
- [19] D.S. Bowden, J.A. Mynderse, From industry to the classroom: A low-cost hardware-in-loop simulator for classic controls experiments, in: 2019 ASEE Annual Conference & Exposition, No. 10.18260/1-2–32864, ASEE Conferences, Tampa, Florida, 2019.
- [20] S.A. Esteban, H.D. Lopez Jr., P. Nolan Tsuchiya, P. Mannion, Low-cost open-architecture experimental platform for dynamic systems and feedback control, in: 2021 ASEE Virtual Annual Conference Content Access, No. 10.18260/1-2–37469, ASEE Conferences, Virtual Conference, 2021.
- [21] R.F. Richards, F.S. Meng, F.L.S. Bernard J. Van Wie, A.L. Ivory, MAKER: Very low-cost experiments via 3-D printing and vacuum forming, in: 2015 ASEE Annual Conference & Exposition, No. 10.18260/p.24458, ASEE Conferences, Seattle, Washington, 2015.
- [22] F. Meng, V.W.B. J. D.B. Thiessen, R.F. Richards, Design and fabrication of very-low-cost engineering experiments via 3-D printing and vacuum forming, *Int. J. Mech. Eng. Educ.* 47 (3) (2019) 246–274.
- [23] F.L. Lewis, D. Vrabie, V.L. Syrmos, *Optimal Control*, John Wiley & Sons, 2012.
- [24] L. Pedroso, P. Batista, Discrete-time decentralized linear quadratic control for linear time-varying systems, *Internat. J. Robust Nonlinear Control* 1–35, <http://dx.doi.org/10.1002/rnc.5772>.